Effects of an Erbium:Yttrium-Aluminum-Garnet Laser and Ultrasonic Scaler on Titanium Dioxide-Coated Titanium Surfaces Contaminated With Subgingival Plaque: An In Vitro Study to Assess Post-Treatment Biocompatibility With Osteogenic Cells

Marco Giannelli,* Daniele Bani,† Alessia Tani,† Fabrizio Materassi,* Flaminia Chellini,† and Chiara Sassoli†

Background: Effects of conventional ultrasonic scaler versus an erbium:yttrium-aluminum-garnet (Er:YAG) laser on titanium surfaces contaminated with subgingival plaque from patients with peri-implantitis are evaluated in terms of: 1) plaque and biocorroded titanium oxide coating removal; 2) surface change induction; and 3) residual biocompatibility toward osteoblasts.

Methods: Subgingival plaque-coated titanium disks with a moderately rough surface were fixed with ethanol and treated with an ultrasonic scaler (metal tip) or Er:YAG laser (20.3 or 38.2 J/cm^2) in non-contact mode. Fluorescent detection of residual plaque was performed. Disk surface morphology was evaluated by scanning electron microscopy. Viability, attachment, proliferation, and differentiation of Saos-2 osteoblasts on new and treated disks were assayed by propidium iodide/DNA stain assay and confocal microscopic analysis of cytoskeleton, Ki67, expression of osteopontin and alkaline phosphatase, and formation of mineralized nodules.

Results: Both methods resulted in effective debridement of treated surfaces, the plaque area being reduced to 11.7% with the ultrasonic scaler and ≤0.03% with the Er:YAG laser (38.2 J/cm^2). Ultrasound-treated disks showed marked surface changes, incomplete removal of the titanium dioxide (TiO_2) layer, and scanty plaque aggregates, whereas the Er:YAG laser (38.2 J/cm^2) completely stripped away the plaque and TiO_2 layer, leaving a micropitted surface. Both treatments maintained a good biocompatibility of surfaces to Saos-2 osteoblasts. Air-water cooling kept disk temperature below the critical threshold of 47°C.

Conclusion: This study shows that an ultrasonic scaler with metal tip is less efficient than high-energy Er:YAG irradiation to remove the plaque and TiO_2 layer on anodized disks, although both procedures appear capable of restoring an adequate osseoconductivity of treated surfaces. *J Periodontol 2017;88:1211-1220.*

KEY WORDS

Dental implants; dental scaling; histocompatibility; lasers, solid state; peri-implantitis.

* Odontostomatologic Laser Therapy Center, Florence, Italy.
† Department of Experimental and Clinical Medicine, Section of Anatomy and Histology, University of Florence, Florence, Italy.

doi: 10.1902/jop.2017.170195

Use of titanium dental implants has deeply transformed the replacement of teeth lost due to disease, injury, or congenital tooth agenesis because of its good strength, resistance to corrosion, excellent biocompatibility, and negligible direct proinflammatory effects.[1] Implant surface morphology and chemistry have been demonstrated to influence adhesion of osteogenic cells both in vitro and in vivo.[2] Several studies have suggested that a porous phosphate-enriched titanium dioxide (TiO_2) surface increases electrochemical corrosion resistance of alloys[3-5] and enhances osseointegration.[6,7] Despite the ever-increasing rate of success, some implants still fail due to peri-implantitis, even after years of successful osseointegration.[8] Peri-implantitis, one of the most severe complications of implant therapy, has been related to bacterial contamination covering almost 60% of the implant and hindering reattachment of bone cells to the surface.[9] Bacterial biofilm and acidic food can lead to localized chemical changes of the crevicular environment induced by poor aeration and oxygen depletion and consisting of significant pH decrease, which, in turn, cause metal bulk attack and degradation/corrosion of the TiO_2 surface coating.[10-13] Corrosion byproducts can affect biocompatibility and function of dental implants and induce an inflammatory reaction or foreign-body reactions.[14,15] This can result in release of inflammatory mediators from macrophages, which activate osteoclasts and contribute to bone resorption and implant failure.[14,15] Therefore, efficient implant debridement methods should ideally remove not only plaque, hard deposits, and bacterial proinflammatory factors but also the altered TiO_2 coating, thereby re-creating a biologically acceptable, osseoconductive surface.[16]

Several methods are in use for decontamination of the implant surface, such as air-powered abrasive treatments, citric acid, and mechanical cleaning by metal or plastic curets or piezoelectric ultrasonic scalers,[5,17] alone or in combination with chemotherapeutic/antiseptic agents.[18,19] However, none of these methods have emerged as perfectly suitable to eliminate bacteria, debris, and corroded TiO_2 from surfaces of implants[8] and to render them biologically permissive to bone regeneration and reosseointegration.[18] In the last decade, the excellent effects of laser light for cleaning and decontamination of implant surfaces have been reported.[20-22] Various laser systems are in use for these purposes, namely CO_2, neodymium: yttrium-aluminum-garnet, erbium:yttrium-aluminum-garnet (Er:YAG), and diode lasers.[23-25] Among them, some studies have pointed to the Er:YAG laser as the most promising method for implant surface cleaning and induction of bone regeneration.[26,27] However, effects of laser irradiation on implant surfaces are known only in part because they depend on many interconnected variables, such as wavelength, irradiation parameters, and implant surface characteristics. This represents an obstacle to definition of a widely accepted, standard treatment protocol for peri-implantitis. For instance, although rough implant surfaces are usually endowed with superior osseointegration, it has been demonstrated that plaque biofilm adheres more strongly to rough rather than smooth implant finishes.[28]

The purpose of this in vitro study is to investigate the effects of a conventional ultrasonic scaler with metal tip compared with an Er:YAG laser on subgingival plaque-coated titanium substrates similar to dental implants, in terms of: 1) removal of plaque and TiO_2 layer; 2) induction of morphologic and thermal changes of treated surfaces; and 3) biocompatibility with osteoblasts (viability, adhesion, proliferation, and differentiation).

The null hypothesis to disprove is that both treatments have similar effects on the treated surface and that removal of the surface TiO_2 layer adversely affects biocompatibility.

MATERIALS AND METHODS

Sample Preparation

Disks‡ made from commercially pure titanium (grade 4), with 6-mm diameter, 2-mm thickness, and rough TiO_2 surface (7- to 10-μm thick) similar to commercial dental implants, were used for the experiments. Samples of bacterial plaque were taken from six patients (four males and two females, aged 35 to 65x years; mean age: 50.8 years) with at least two implants with peri-implantitis. Patients enrolled from November 2015 to February 2016 and gave written consent to sampling for the purposes of this study. The study was conducted in accordance with the Helsinki Declaration of 1975, as revised in 2000. Peri-implantitis was diagnosed when implants presented mucosal inflammation with or without ≥2 mm of bone loss after restoration, according to the criteria of the Consensus Report of the Sixth European Workshop on Periodontology.[29] Bacterial plaque was taken from the subgingival margin of diseased implants with sterile curets, the edge away from the implant surfaces, and smeared on the upper surface of the disks.[15] The disks were fixed for 10 minutes in 95% ethanol to simulate hardened plaque,[30] allowed to dry, and kept at 4°C in sterile microtubes until use. A total of 28 plaque-coated disks and 14 uncoated control disks were used for the experiments.

Ultrasonic Scaler and Er:YAG Laser Treatment

An experienced periodontist (MG) performed treatment of the disks using two different procedures: 1) ultrasonic scaler apparatus§ equipped with a P4

‡ TiUnite, Nobel Biocare AB, Gothenburg, Sweden.
§ Multipiezo Pro, Mectron, Genova, Italy.

Table 1.

Er:YAG Laser Irradiation Parameters

Parameter	Value	
Wavelength (nm)	2,940	
Irradiation mode	Pulsed wave	
Frequency (Hz)	12	
Tip diameter (HPX conical) (μm)	200	
Treatment time (seconds)	60	
Pulse width (μs)	400	
Tip speed (mm/seconds)	2.5	
Treatment mode	Non-contact	
Tip-target gap (mm)	0.5	
Spot diameter (mm)	0.35	
Spot area at target level (mm^2)	0.4	
Pulse energy (mJ)	80	150
Pulse power density (W/cm^2)	244.46	458.37
Pulse fluence (J/cm^2)	20.37	38.2

steel tip and set at 50% of full power at high frequency (36 kHz) for 1 minute under water flow cooling (28 mL/minute). The tip was positioned approximately perpendicular to the specimen and moved from the periphery to the center of disk with a constant force of about 30 g; and 2) Er:YAG laser‖ operating at λ 2,964 nm for 1 minute in non-contact mode, keeping the tip 0.5 mm from the disk surface with an angle of 90 degrees. The handpiece was moved with a constant speed of 2 mm/second from the periphery to the center of the disks under air/water flow cooling. Two different output energy settings, 80 or 150 mJ/12 Hz corresponding to a pulse fluence of 20.3 and 38.2 J/cm^2, respectively, were used, based on those used clinically on implant surfaces,[27,31] as detailed in Table 1. Before irradiation, output energy at the extremity of the conical tip was measured with a power meter to assess possible deviation from the value indicated on the laser console. Disk temperature was recorded before and during the treatments using an infrared-thermal camera.¶

Fluorescent Detection of Residual Bacterial Plaque

Plaque-coated disks, untreated (controls) or treated with ultrasonic scaler or Er:YAG laser (for each group, n = 3), were stained for 2 minutes at 37°C with a fluorescent cell viability stain# to detect residual bacterial plaque.[32] After thorough rinsing in distilled water, disks were mounted on a glass slide and observed under an epifluorescence light microscope equipped with a digital camera.** Digital images of six microscopic fields (magnification ×40, test area 61,275 μm^2 per field) were taken from each disk, and the surface area of the fluorescent residual plaque was measured by a trained morphologist (DB), masked to the treatments, using image analysis software.†† Measurements are expressed as percentage of the test area, assumed as 100%.

Scanning Electron Microscopy (SEM)

To analyze in detail the surface morphology before and after different treatments, some disks (n = 1 each group) were rinsed with distilled water, dehydrated in acetone, passed through hexamethyldisilazane, sputter-coated with platinum (10 nm), and examined with SEM.‡‡ An experienced observer (DB), masked to the experimental conditions, carried out the ultrastructural analysis.

Osteoblastic Cell Cultures

Plaque-coated disks treated with either ultrasonic scaler or Er:YAG laser (150 mJ/cm^2) were sterilized by autoclavation before use. Uncoated, untreated disks served as controls (each experiment, n = 2 per group). Human osteoblast-like Saos-2 cells§§ were cultured in growth medium containing F12-Coon modification medium supplemented with 10% fetal bovine serum, 1% glutamine, and 100 U/mL penicillin-streptomycin. Preconfluent cells were harvested and seeded in a drop of medium (2×10^4 in 25 μL) over the disks, placed individually into a 12-well multiplate. Cells were allowed to adhere to disks for 1 hour before addition of further growth medium into the wells and cultured for 24 hours. Cells were shifted to osteogenic differentiation medium supplemented with 100 μg/mL ascorbic acid, 10 mM β-glycerophosphate, and 10 nM dexamethasone and cultured for 7 and 14 days. The differentiation medium was replaced every 3 to 4 days. All reagents were obtained from the same manufacturer.‖‖

Confocal Laser Scanning Microscopy

Cells cultured on disks for 24 hours or 7 or 14 days were fixed with 0.5% buffered paraformaldehyde for 10 minutes at room temperature, permeabilized with cold acetone for 3 minutes, blocked with a solution containing 0.5% bovine serum albumin and 3% glycerol

‖ Opus Duo EC, Lumenis, Milan, Italy.
¶ Flir One, Flir, Meer, Belgium.
# LIVE/DEAD BacLight, Thermo Fisher Scientific, Waltham, MA.
** Leica 4000 B, Leica Microsystems, Milan, Italy.
†† ImageJ v1.42q image analysis software, National Institutes of Health, Bethesda, MD.
‡‡ Supra 40VP, Zeiss, Oberkochen, Germany.
§§ ATCC, Manassas, VA.
‖‖ Sigma-Aldrich, St. Louis, MO.

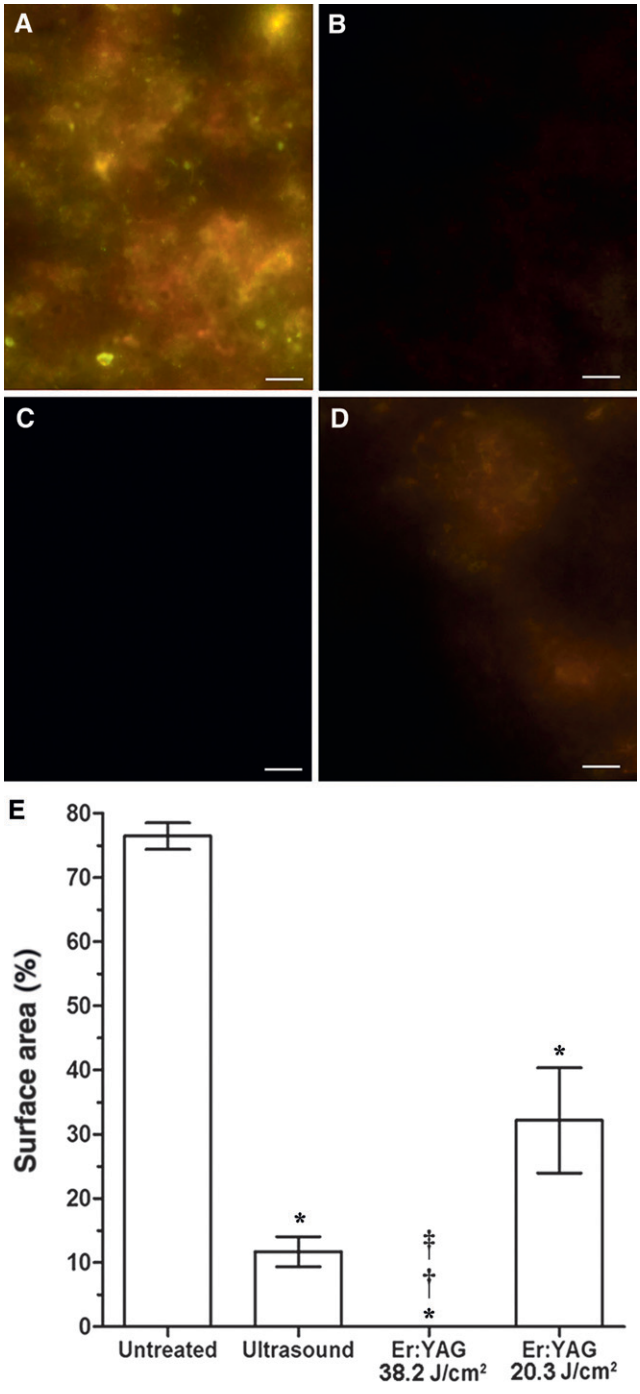

Figure 1.
A through D) *Bacterial plaque removal assessed by fluorescent viability staining. (original magnification ×400; bars = 100 μm). A) Untreated plaque-coated disk. B) Disk treated with ultrasonic scaler. C) Disk treated with Er:YAG laser at 38.2 J/cm². D) Disk treated with Er:YAG laser at 20.3 J/cm².* ***E)*** *Plaque area calculated as percentage of test area (microscopic field). Statistical analysis: one-way ANOVA and Newman-Keuls post-test.* *P <0.001 *versus untreated;* †P <0.001 *versus ultrasonic treatment;* ‡P <0.001 *versus treatment with Er:YAG at 20.3 J/cm².*

in phosphate-buffered saline (PBS) for 20 minutes, and incubated overnight at 4°C with rabbit polyclonal antiKi67¶¶ (1:100). This was done to evaluate cycling cells (24 hours), antiosteopontin## (1:50), and alkaline phosphatase (1:200)*** to assess osteoblastic differentiation (7 days). Immune reactions were revealed by antirabbit fluorochrome, 488 nm or 588 nm wavelength-conjugated IgG††† (1:200) for 1 hour at room temperature. In some experiments, cells were stained with a fluorescent actin stain (1:40)‡‡‡ to detect actin filament organization. In other experiments counterstaining with propidium iodide§§§ (PI, 1:30) was performed to reveal nuclei and count cells. Negative controls were carried out by replacing primary antibodies with non-immune serum; cross-reactivity of secondary antibodies was tested in control experiments in which primary antibodies were omitted. Cell viability was assayed with the PI exclusion test on cells grown over disks in osteogenic differentiation medium (24 hours). After medium removal, cells were incubated for 15 minutes at 37°C in PBS containing PI (1:100) and a DNA stain‖‖ (1:200), washed in PBS, fixed in 0.5% paraformaldehyde, and observed at the confocal microscope. In each cell preparation, the number of PI-stained nuclei (dead cells) was evaluated in at least 10 random microscopic fields, 40,000 μm² each, and expressed as percent total cells.

After labeling, disks were placed on glass coverslips and observed under a confocal microscope¶¶¶ equipped with an HeNe/Ar laser source for fluorescence measurements. Observations were performed using an oil immersion objective.### A series of optical sections (1,024 × 1,024 pixels each; pixel size, 204 nm) were taken through the depth of the cells at intervals of 0.4 μm. Images were superimposed to form a single extended-focus image. In each specimen, the percentage of Ki67 nuclei over total nuclei was evaluated in 10 random microscopic fields, 40,000 μm² each, by two independent observers (FC and CS), and measurements were averaged; experiments were performed in triplicate. Densitometric analysis of the extension of osteopontin and alkaline phosphatase fluorescence was performed on digitized images using the appropriate software**** in 20 regions of interest (ROIs) of 100 μm² for each confocal stack (at least 10).

¶¶ Abcam, Cambridge, U.K.
Santa Cruz Biotechnology, Santa Cruz, CA.
*** Clone TRA-2-54/2J, Millipore, Temecula, CA.
††† Alexa Fluor 488- or 568-conjugated IgG, clone TRA-2-54/2J, Millipore.
‡‡‡ Alexa Fluor 488-labeled phalloidin, Thermo Fisher Scientific.
§§§ Molecular Probes, Eugene, OR.
‖‖ SYTO 9, Thermo Fisher Scientific.
¶¶¶ TCS SP5 microscope, Leica Microsystems, Mannheim, Germany.
Plan Apo ×63/1.43 NA oil immersion objective, Leica Microsystems.
**** ImageJ v1.42q image analysis software, National Institutes of Health.

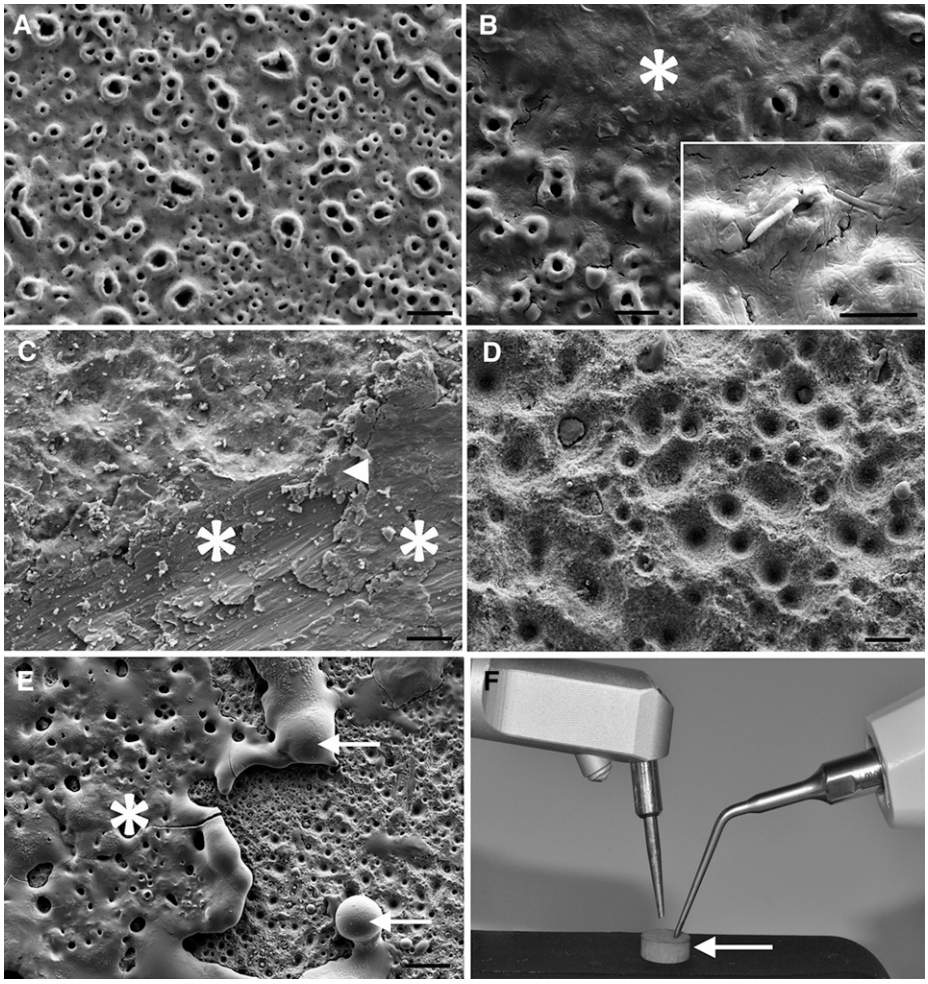

Figure 2.
A through E) *Representative SEM micrographs of disk surface morphology (original magnification ×1,000; bars = 10 μm). A) Uncoated, untreated titanium disk. B) Plaque-coated, untreated disk showing a thick layer of bacterial plaque (asterisk and inset). C) Plaque-coated disk treated with ultrasound showing a markedly flattened surface with scraping grooves (asterisks) and remnants of the TiO_2 layer and plaque (arrowhead). D) Plaque-coated disks treated with Er:YAG laser (38.2 J/cm^2) showing complete removal of plaque and surface TiO_2 layer and exposure of a micropitted surface. E) Plaque-coated disks treated with Er:YAG laser (20.3 J/cm^2) showing persistence of large parts of the surface TiO_2 layer (asterisk) with marginal microfusions (arrows) adjacent to micropitted titanium areas (right).* ***F)*** *Close view of a titanium disk (arrow) and of the handpieces of the Er:YAG laser (left) and the ultrasound with metal tip (right).*

Fluorescent Mineralized Nodules Assay

Formation of mineralized nodules by Saos-2 cells, a functional marker of mature osteoblasts, was detected by a fluorescent assay.†††† This reagent selectively binds to hydroxyapatite in bone-like nodules deposited by cells. Briefly, Saos-2 cells cultured for 14 days in osteogenic differentiation medium on disks pretreated as reported above, were fixed with 0.5% paraformaldehyde, rinsed twice in the provided buffer and then incubated with the staining reagent for 30 minutes at room temperature in the dark. After thorough rinsing, the specimens were observed under the confocal laser scanning microscope. Densitometric analysis of the intensity of the fluorescent signal was performed on digitized images using the ImageJ software in 20 ROIs of 100 μm^2 for each confocal stack (at least 10).

Statistical Analyses

Values are expressed as mean ± SEM of at least three independent experiments carried out in triplicate. Statistical analysis of differences between the experimental groups was performed using one-way analysis of variance (ANOVA) followed by Newman-Keuls multiple comparison test. Differences were considered statistically significant when $P \leq 0.05$. Calculations were performed using statistical software.‡‡‡‡

RESULTS

Bacterial Plaque Removal

Compared with untreated plaque-coated disks (controls), both the ultrasonic scaler and Er:YAG laser procedures resulted in almost complete debridement of treated surfaces. The residual plaque area was reduced from 76.5% ± 2.1% in the untreated controls to 11.7% ± 2.3% in disks treated with ultrasonic scaling and to 32.2% ± 8.2% and 0.03% ± 0.001% in disks treated with Er:YAG laser set at 20.3 and 38.2 J/cm^2, respectively (all treatments: $P < 0.001$ versus controls). Morphologically, the almost continuous fluorescent plaque coat seen in the untreated controls was reduced to small, sparse clumps on ultrasonic or low-power laser treatments and nearly disappeared on high-power laser treatment (Fig. 1).

Infrared-thermal measurements showed a 26°C ± 2°C baseline temperature (time 0). After 60 seconds of treatment with the ultrasonic scaler, the temperature rose to 44°C ± 5°C with no cooling and 29°C ± 7°C with water spray cooling. The temperature was uniformly distributed on the disk surface. After 60 seconds of irradiation with an Er:YAG laser at 20.3 J/cm^2, the temperature was 46°C ± 9°C with no

†††† Osteolmage, Lonza, Walkersville, MD.
‡‡‡‡ Prism v4.0, GraphPad, San Diego, CA.

cooling and 29°C ± 2°C with air and water cooling. Using the 38.2 J/cm^2 setting, the temperature was 58°C ± 7°C with no cooling and 30°C ± 5°C with air and water cooling.

Alterations of Titanium Surface Morphology

By SEM analysis, the surface of the uncoated, untreated titanium disks (Fig. 2A) was characterized by a peculiarly shaped TiO_2 layer with numerous microcavities, intended for favoring colonization by cells of the peri-implant tissues and increasing osseoconductivity. The plaque-coated, untreated disks (Fig. 2B) showed an adherent layer of closely packed bacteria of various shapes, embedded in a filamentous matrix that almost completely filled the microcavities of the titanium surface. Plaque-coated disks treated with an ultrasonic scaler with a metal tip showed a markedly flattened surface with scraping grooves and the disappearance of microcavities, but with incomplete removal of the TiO_2 layer and scanty aggregates of plaque-like material (Fig. 2C). Plaque-coated disks treated with Er:YAG laser set at 38.2 J/cm^2 showed that both the plaque and surface of the TiO_2 layer were completely stripped away, leaving a micropitted titanium surface. Of note, this surface showed no signs of melting or other heat-induced deformation (Fig. 2D). On the other hand, the Er:YAG laser set at 20.3 J/cm^2 showed little residual plaque but large remnants of surface TiO_2 layer intermingled with areas of clean, micropitted titanium surface (Fig. 2E). The two handpieces and the disk are also shown in Figure 2F.

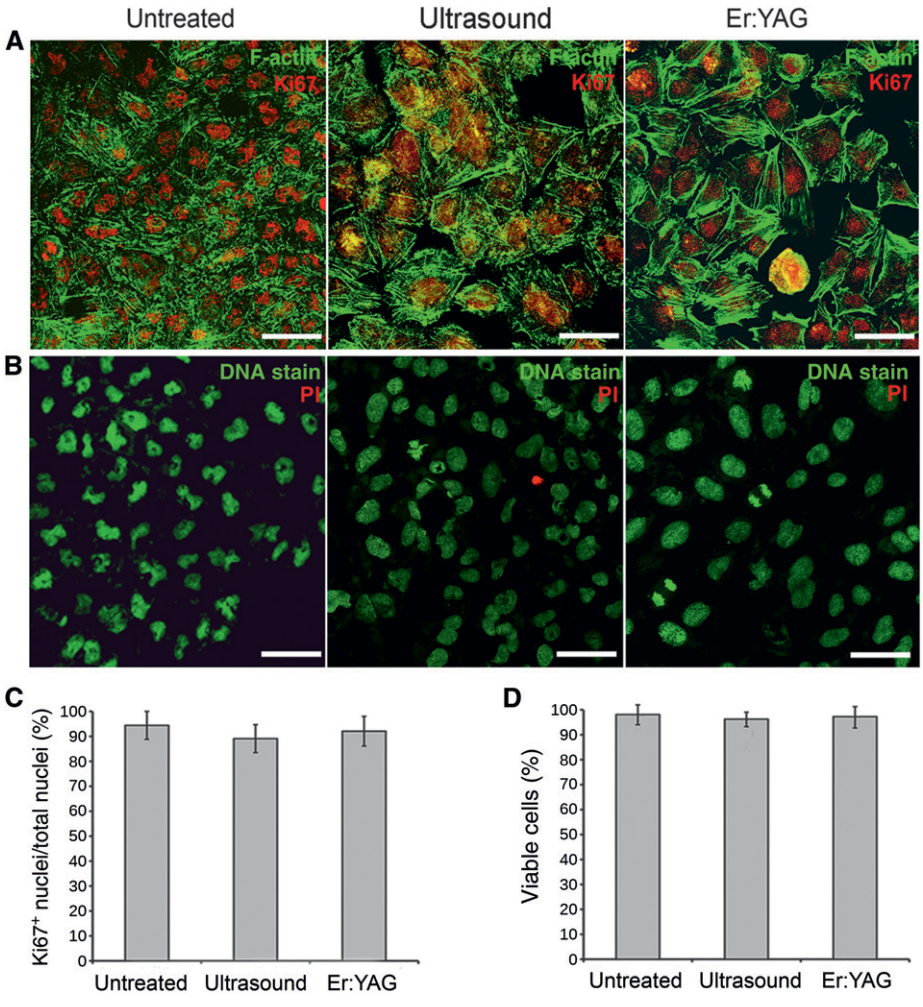

Figure 3.
A *and* ***B)*** *Representative confocal fluorescence micrographs of Saos-2 osteoblasts grown for 24 hours on untreated, uncoated control disks (left row); plaque-coated, ultrasound-treated disks (center row); and plaque-coated, Er:YAG laser-treated (38.2 J/cm^2) disks (right row) (original magnification ×200; bars = 50 μm). A) Double labeling for Ki67 cycling cell antigen and F-actin cytoskeleton, mostly arranged in stress fibers typical of substrate-adherent cells. B) Nuclear staining for viable (DNA stain) and dead (PI) cells.* ***C*** *and* ***D)*** *Morphometric analysis of percentage of total cells of Ki67-positive and PI-positive cells. Differences among the groups were not significant (one-way ANOVA and Newman-Keuls post-test).*

Biocompatibilty With Osteoblasts

Confocal fluorescence examination of Saos-2 osteoblasts grown on untreated disks for 24 hours showed that a majority of the cells expressed the Ki67 nuclear proliferation marker, typical of cycling cells; exhibited a well-developed cytoskeletal framework of actin stress fibers, typical of substrate-adherent cells; and were mostly negative to nuclear PI staining, a marker of dead cells. Similar features were observed in the plaque-coated disks subjected to debridement with either ultrasonic scaler or Er:YAG laser (38.2 J/cm^2), indicating that the observed surface alterations did not substantially compromise osteoblastic cell growth, adhesion, and viability (Fig. 3).

Evaluation and quantification of the expression of osteopontin, alkaline phosphatase, and Ca^{2+} deposits (Fig. 4), assumed as osteoblast differentiation markers, showed that compared with untreated disks, the ultrasonic scaler and Er:YAG laser did not cause substantial changes of the

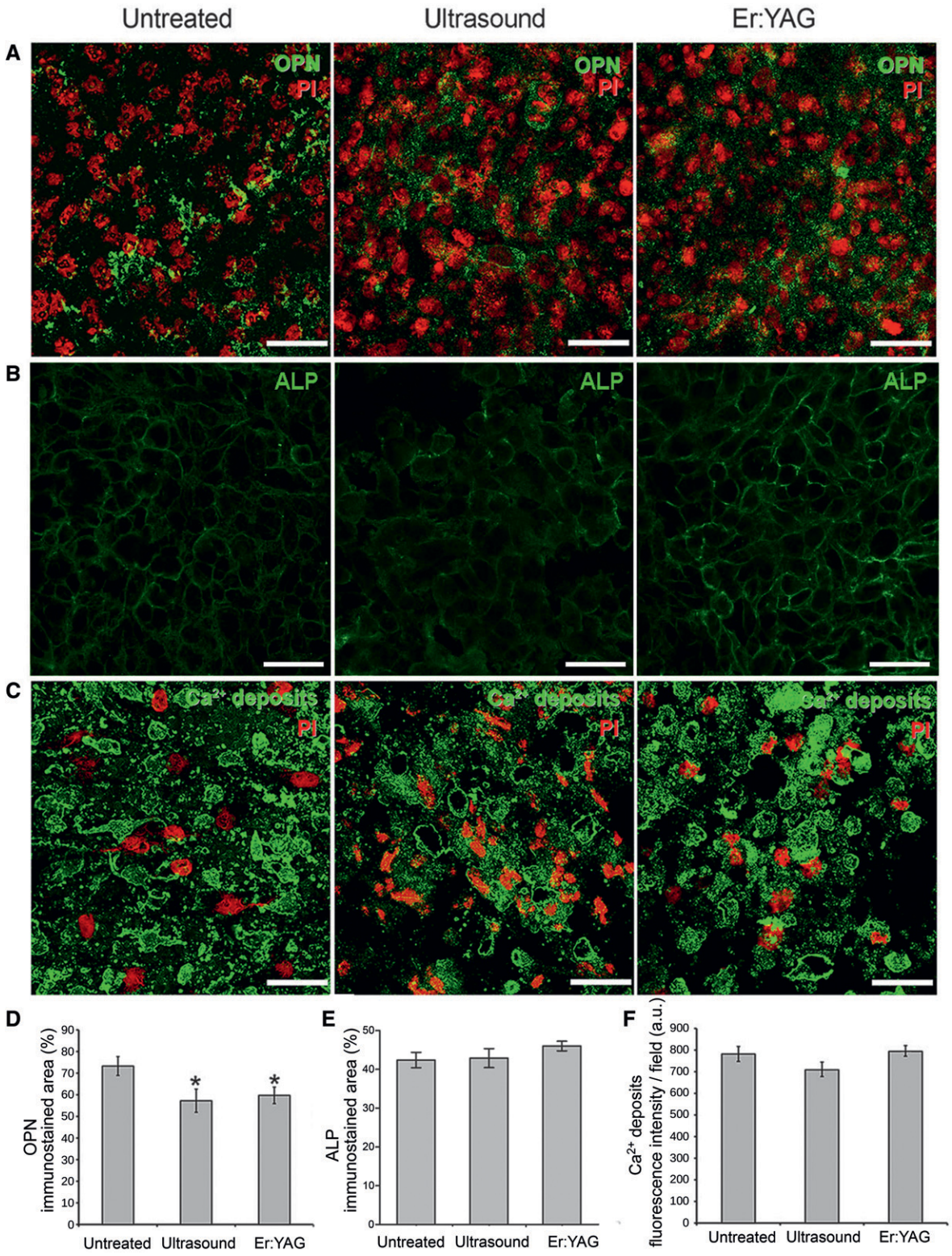

Figure 4.

A through C) *Representative confocal fluorescence micrographs of Saos-2 osteoblasts grown for 7 or 14 days on untreated, uncoated control disks (left row), plaque-coated, ultrasound-treated disks (center row), and plaque-coated, Er:YAG laser-treated (38.2 J/cm^2) disks (right row). (Original magnification ×200; bars = 50 μm.) Immunolabeling for osteoblast differentiation markers (7 days): A) osteopontin (OPN); B) alkaline phosphatase (ALP); C) fluorescent labeling of mineralized nodules (Ca^{2+} deposits) with fluorescent dye (14 days).* ***D through F)*** *Morphometric analysis of OPN and ALP immunolabeled areas and of fluorescent Ca^{2+} deposits. Significance of differences (one-way ANOVA and Newman-Keuls post-test):* *P *<0.05 versus untreated controls. a.u. = arbitrary units.*

expression of these markers, except for a slight—albeit statistically significant—reduction for osteopontin. The Er:YAG laser set at suboptimal energy output (20.3 J/cm^2) left too much bacterial plaque to allow Saos-2 cell attachment and culture. The negative controls showed no fluorescence.

DISCUSSION

Peri-implant bacterial contamination and bio-corrosion are etiologic factors in the pathogenesis of peri-implantitis.[15] It has been recently assessed that bacterial byproducts can alter the physicochemical composition of a titanium surface, causing disruption of the TiO_2 layer and titanium dissolution.[15,16,33] These emerging concepts suggest that a correct therapeutic approach to peri-implantitis should meet the requirements of eliminating bacterial plaque as well as the corroded TiO_2 surface, which can adversely influence osteoblast adhesion and growth,[16] the prerequisite for bone formation and reosseointegration. Mechanical implant surface debridement has long been the gold standard in peri-implantitis therapy,[17] but information is incomplete about how these treatments can affect biocompatibility of the implant toward peri-implant bone cells, especially for implants with complex surface characteristics, such as anodized TiO_2 implants.[34,35] Moreover, it has been shown that some instruments used for implant debridement can smear deposits of the same material as the instrument tip over treated surfaces, thereby disturbing cell attachment.[36]

Results of the present study show that implant debridement achieved by means of mechanical ultrasonic scaler with a metal tip or Er:YAG laser yields different effects on the removal of bacterial plaque and surface TiO_2. Of these treatments, the efficacy of the high-power Er:YAG laser (38.2 J/cm^2) was superior to the ultrasonic scaler since it was able to completely remove the plaque coat as well as the purportedly biocorroded TiO_2 surface, leaving a micropitted interface biocompatible with osteoblastic cells. These findings are in accordance with previous in vivo studies demonstrating the capability of the Er:YAG laser to decontaminate implant surfaces by stripping the TiO_2 layer and providing a clean surface suitable for bone regeneration.[27,31] Conversely, the ultrasonic scaler, albeit handled by an expert operator, left about 11.7% of residual plaque and sparse TiO_2 debris on the treated surface. Of note, efficiency of ultrasonic scaling depends on many factors, such as design, tip material, vibration frequency, power, water flow rate, contact angle, and load.[37] Peculiarly, when the Er:YAG laser was set at a relatively low energy output (20.3 J/cm^2), it lost most of its efficacy, leaving 32.2% of the plaque and large areas of the TiO_2 coating. Presence of bacterial plaque remnants is particularly dangerous as it may predispose the implant to bacterial regrowth. Of note, although both the ultrasonic scaler with metal tip and Er:YAG laser (38.2 J/cm^2) induced marked surface alterations of titanium disks, the cell culture experiments indicate that none of them actually impaired the capability of Saos-2 osteoblastic cells to adhere and proliferate. Indeed, Saos-2 cells grown on disks pretreated with either method were observed to maintain a high proliferative potential, as argued by the high percentage of Ki67-positive nuclei similar to that of the untreated, new control disks specifically designed to be osseoconductive. These cells were also able to adhere to treated surfaces, as suggested by the three-dimensional assembly of their actin cytoskeleton needed to stabilize focal adhesions,[38] and to properly respond to differentiation stimuli toward mature bone-producing cells. In fact, incubation of Saos-2 cells with osteogenic differentiation medium induced expression of osteopontin and alkaline phosphatase (7 days), typical osteoblastic markers,[39] followed by deposition of mineralized Ca^{2+} containing clumps (14 days). Compared with untreated control disks, those subjected to ultrasonic scaler or laser debridement appeared to slightly hinder osteoblastic cell differentiation, although differences only reached statistical significance for osteopontin expression, not for alkaline phosphatase or mineralization ability. The reasons for this discrepancy remain elusive. It could be hypothesized that the induced alterations of the original rough TiO_2 surface optimized for osseoconductivity had resulted in abnormal adhesion-derived signals capable of impairing some cell differentiation pathways.

These findings confute the null hypothesis that the two methods would be equally detrimental for surface biocompatibility. However, it must be underlined that the Er:YAG laser at suboptimal energy output (20.3 J/cm^2) was nearly ineffective, in keeping with the emerging concept that a proper, accurate tuning of dental lasers is needed to achieve the desired therapeutic effects.[36]

To avoid temperature increases beyond the tissue-damage threshold of 47°C, ultrasonic scaling should be performed with proper air cooling, and the Er:YAG laser requires dual air and water cooling. These results agree with previous reports[40] and confirm the importance of cooling during Er:YAG laser and ultrasonic treatment of dental implants.[41,42]

Some major limitations of this in vitro study are to be considered when translating the present in vitro data to dental practice: 1) observed effects of the two debridement methods were tested on titanium disks with the same microporous osseoconductive surface as dental implants but with different macrotopography and not interlocked with peri-implant

bone; and 2) Saos-2 cells are a tumor-derived cell line and may not behave as true osteoblasts in vivo. In fact, in clinical practice, effective treatment of dental implant surfaces can be substantially more difficult to achieve, especially with the ultrasonic scaler, which must be maneuvered in infrabony areas all around the implant in contact mode. To this purpose, the Er:YAG laser, which is used in non-contact mode, offers an additional handling advantage on the complicated structure of the implant threads. It also should be taken into account that treated disks used in this study had to be autoclaved before being used for the cell culture experiments. This treatment may have influenced the surface composition of titanium, favoring the *de novo* formation of TiO_2,[43] which is known to be necessary for implant biocompatibility. These limitations dictate caution if the present findings will be used as background for new clinical protocols.

CONCLUSION

The present study offers circumstantial evidence that an ultrasonic scaler with a metal tip is less efficient than high-energy Er:YAG irradiation to remove plaque and the TiO_2 layer on anodized implants, although both procedures appear capable of restoring adequate osseoconductivity of the treated surfaces.

ACKNOWLEDGMENTS

The authors thank Dr. Peter Schüpbach, from Schüpbach (Thalwil, Switzerland) for conducting the SEM investigation and to Nobel Biocare AG (Zürich, Switzerland) for providing the TiO_2-coated disks. Funding was not sought or obtained for execution of the project. The authors report no conflicts of interest related to this study.

REFERENCES

1. Bächle M, Kohal RJ. A systematic review of the influence of different titanium surfaces on proliferation, differentiation and protein synthesis of osteoblast-like MG63 cells. *Clin Oral Implants Res* 2004;15:683-692.
2. Monjo M, Lamolle SF, Lyngstadaas SP, Rønold HJ, Ellingsen JE. In vivo expression of osteogenic markers and bone mineral density at the surface of fluoride-modified titanium implants. *Biomaterials* 2008;29:3771-3780.
3. Rocci A, Martignoni M, Gottlow J. Immediate loading of Brånemark System TiUnite and machined-surface implants in the posterior mandible: A randomized open-ended clinical trial. *Clin Implant Dent Relat Res* 2003;5(Suppl. 1):57-63.
4. Simon M, Lagneau C, Moreno J, Lissac M, Dalard F, Grosgogeat B. Corrosion resistance and biocompatibility of a new porous surface for titanium implants. *Eur J Oral Sci* 2005;113:537-545.
5. Park JB, Jang YJ, Koh M, Choi BK, Kim KK, Ko Y. In vitro analysis of the efficacy of ultrasonic scalers and a toothbrush for removing bacteria from resorbable blast material titanium disks. *J Periodontol* 2013;84:1191-1198.
6. Xiropaidis AV, Qahash M, Lim WH, et al. Bone-implant contact at calcium phosphate-coated and porous titanium oxide (TiUnite)-modified oral implants. *Clin Oral Implants Res* 2005;16:532-539.
7. Sawase T, Jimbo R, Wennerberg A, Suketa N, Tanaka Y, Atsuta M. A novel characteristic of porous titanium oxide implants. *Clin Oral Implants Res* 2007;18:680-685.
8. Polizzi G, Gualini F, Friberg B. A two-center retrospective analysis of long-term clinical and radiologic data of TiUnite and turned implants placed in the same mouth. *Int J Prosthodont* 2013;26:350-358.
9. Salvi GE, Cosgarea R, Sculean A. Prevalence and mechanisms of peri-implant diseases. *J Dent Res* 2017;96:31-37.
10. Olmedo DG, Tasat DR, Duffó G, Guglielmotti MB, Cabrini RL. The issue of corrosion in dental implants: A review. *Acta Odontol Latinoam* 2009;22:3-9.
11. Gil FJ, Rodriguez A, Espinar E, Llamas JM, Padullés E, Juárez A. Effect of oral bacteria on the mechanical behavior of titanium dental implants. *Int J Oral Maxillofac Implants* 2012;27:64-68.
12. Olmedo DG, Nalli G, Verdú S, Paparella ML, Cabrini RL. Exfoliative cytology and titanium dental implants: A pilot study. *J Periodontol* 2013;84:78-83.
13. Sridhar S, Abidi Z, Wilson TG Jr., et al. In vitro evaluation of the effects of multiple oral factors on dental implants surfaces. *J Oral Implantol* 2016;42:248-257.
14. Sridhar S, Wilson TG Jr., Palmer KL, et al. In vitro investigation of the effect of oral bacteria in the surface oxidation of dental implants. *Clin Implant Dent Relat Res* 2015;17(Suppl. 2):e562-e575.
15. Safioti LM, Kotsakis GA, Pozhitkov AE, Chung WO, Daubert DM. Increased levels of dissolved titanium are associated with peri-implantitis — A cross-sectional study. *J Periodontol* 2017;88:436-442.
16. Barão VA, Yoon CJ, Mathew MT, Yuan JC, Wu CD, Sukotjo C. Attachment of *Porphyromonas gingivalis* to corroded commercially pure titanium and titanium-aluminum-vanadium alloy. *J Periodontol* 2014;85:1275-1282.
17. Subramani K, Wismeijer D. Decontamination of titanium implant surface and re-osseointegration to treat peri-implantitis: A literature review. *Int J Oral Maxillofac Implants* 2012;27:1043-1054.
18. Mombelli A. Microbiology and antimicrobial therapy of peri-implantitis. *Periodontol 2000* 2002;28:177-189.
19. Renvert S, Lessem J, Dahlén G, Lindahl C, Svensson M. Topical minocycline microspheres versus topical chlorhexidine gel as an adjunct to mechanical debridement of incipient peri-implant infections: A randomized clinical trial. *J Clin Periodontol* 2006;33:362-369.
20. Mailoa J, Lin GH, Chan HL, MacEachern M, Wang HL. Clinical outcomes of using lasers for peri-implantitis surface detoxification: A systematic review and meta-analysis. *J Periodontol* 2014;85:1194-1202.
21. Giannelli M, Landini G, Materassi F, et al. The effects of diode laser on *Staphylococcus aureus* biofilm and *Escherichia coli* lipopolysaccharide adherent to titanium oxide surface of dental implants. An in vitro study. *Lasers Med Sci* 2016;31:1613-1619.
22. Giannelli M, Landini G, Materassi F, et al. Effects of photodynamic laser and violet-blue led irradiation on *Staphylococcus aureus* biofilm and *Escherichia coli*

lipopolysaccharide attached to moderately rough titanium surface: In vitro study. *Lasers Med Sci* 2017;32:857-864.
23. Park CY, Kim SG, Kim MD, Eom TG, Yoon JH, Ahn SG. Surface properties of endosseous dental implants after NdYAG and CO_2 laser treatment at various energies. *J Oral Maxillofac Surg* 2005;63:1522-1527.
24. Schwarz F, Nuesry E, Bieling K, Herten M, Becker J. Influence of an erbium, chromium-doped yttrium, scandium, gallium, and garnet (Er,Cr:YSGG) laser on the reestablishment of the biocompatibility of contaminated titanium implant surfaces. *J Periodontol* 2006;77:1820-1827.
25. Giannelli M, Bani D, Tani A, et al. In vitro evaluation of the effects of low-intensity Nd:YAG laser irradiation on the inflammatory reaction elicited by bacterial lipopolysaccharide adherent to titanium dental implants. *J Periodontol* 2009;80:977-984.
26. Schwarz F, Sculean A, Rothamel D, Schwenzer K, Georg T, Becker J. Clinical evaluation of an Er:YAG laser for nonsurgical treatment of peri-implantitis: A pilot study. *Clin Oral Implants Res* 2005;16:44-52.
27. Yamamoto A, Tanabe T. Treatment of peri-implantitis around TiUnite-surface implants using Er:YAG laser microexplosions. *Int J Periodontics Restorative Dent* 2013;33:21-30.
28. Ferreira Ribeiro C, Cogo-Müller K, Franco GC, et al. Initial oral biofilm formation on titanium implants with different surface treatments: An in vivo study. *Arch Oral Biol* 2016;69:33-39.
29. Lindhe J, Meyle J; Group D of European Workshop on Periodontology. Peri-implant diseases: Consensus report of the Sixth European Workshop on Periodontology. *J Clin Periodontol* 2008;35(Suppl. 8):282-285.
30. Simion M, Kim DM, Pieroni S, Nevins M, Cassinelli C. Bacterial biofilm morphology on a failing implant with an oxidized surface: A scanning electron microscope study. *Int J Periodontics Restorative Dent* 2016;36:485-488.
31. Nevins M, Nevins ML, Yamamoto A, et al. Use of Er:YAG laser to decontaminate infected dental implant surface in preparation for reestablishment of bone-to-implant contact. *Int J Periodontics Restorative Dent* 2014;34:461-466.
32. Al-Hashedi AA, Laurenti M, Benhamou V, Tamimi F. Decontamination of titanium implants using physical methods. *Clin Oral Implants Res* 2017;28:1013-1021.
33. Mouhyi J, Dohan Ehrenfest DM, Albrektsson T. The peri-implantitis: Implant surfaces, microstructure, and physicochemical aspects. *Clin Implant Dent Relat Res* 2012;14:170-183.
34. Albouy JP, Abrahamsson I, Persson LG, Berglundh T. Spontaneous progression of ligatured induced peri-implantitis at implants with different surface characteristics. An experimental study in dogs II: Histological observations. *Clin Oral Implants Res* 2009;20:366-371.
35. Albouy JP, Abrahamsson I, Persson LG, Berglundh T. Implant surface characteristics influence the outcome of treatment of peri-implantitis: An experimental study in dogs. *J Clin Periodontol* 2011;38:58-64.
36. Schwarz F, Rothamel D, Sculean A, Georg T, Scherbaum W, Becker J. Effects of an Er:YAG laser and the Vector ultrasonic system on the biocompatibility of titanium implants in cultures of human osteoblast-like cells. *Clin Oral Implants Res* 2003;14:784-792.
37. Lea SC, Walmsley AD. Mechano-physical and biophysical properties of power-driven scalers: Driving the future of powered instrument design and evaluation. *Periodontol 2000* 2009;51:63-78.
38. Livne A, Geiger B. The inner workings of stress fibers-from contractile machinery to focal adhesions and back. *J Cell Sci* 2016;129:1293-1304.
39. Aubin JE, Liu F. The osteoblast lineage. In: Bilezikian JP, Raisz LG, Rodan GA, eds. *Principles of Bone Biology*. San Diego, CA: Academic Press; 1996:51-67.
40. Kreisler M, Al Haj H, d'Hoedt B. Temperature changes at the implant-bone interface during simulated surface decontamination with an Er:YAG laser. *Int J Prosthodont* 2002;15:582-587.
41. Rühling A, Kocher T, Kreusch J, Plagmann HC. Treatment of subgingival implant surfaces with Teflon-coated sonic and ultrasonic scaler tips and various implant curettes. An in vitro study. *Clin Oral Implants Res* 1994;5:19-29.
42. Geminiani A, Caton JG, Romanos GE. Temperature increase during $CO(_2)$ and Er:YAG irradiation on implant surfaces. *Implant Dent* 2011;20:379-382.
43. Khosroshahi ME, Mahmoodi M, Saeedinasab H. In vitro and in vivo studies of osteoblast cell response to a titanium-6 aluminium-4 vanadium surface modified by neodymium:yttrium-aluminium-garnet laser and silicon carbide paper. *Lasers Med Sci* 2009;24:925-939.

Correspondence: Dr. Marco Giannelli, Odontostomatologic Laser Therapy Center, Via dell' Olivuzzo 162, 50143 Florence, Italy. E-mail: dott.giannellimarco@gmail.com.

Submitted March 21, 2017; accepted for publication June 1, 2017.